

Ultrasound generation enhancement with carbon-based nanoparticles as photoacoustic sensitizers

K. Dubyk^{1,2}, A. Kuzmich^{1,2}, M. Isaiev^{1,2}, S. Alekseev^{1,2}

¹ Taras Shevchenko National University of Kyiv
Kyiv, Ukraine

² Science Park Kyiv Taras Shevchenko University
Kyiv, Ukraine

B. Zousman³, O. Levinson³

³ Ray Techniques Ltd
Hebrew University of Jerusalem
Jerusalem, Israel

A. Rozhin⁴

⁴ Aston Institute of Photonic Technologies
Aston University
Birmingham, United Kingdom

V. Lysenko⁵

⁵ Institut des Nanotechnologies de Lyon
Université de Lyon
Villeurbanne, France

Abstract—Laser ultrasound enhancement with carbon-based nanomaterials incorporated into phantom tissues is reported. More specifically, impact of nanodiamonds and graphene oxide on the efficiency of photoinduced pressure excitation was investigated. Agarose-based phantom tissues with and without the nanoparticles were compared. The second harmonic of pulsed Nd:Yag laser (532 nm) was chosen for ultrasound generation. Specific acoustic probe was fabricated for laser-induced ultrasound registration. Dependence of the ultrasound amplitude on concentration of the nanoparticles incorporated into the phantom tissues was analyzed in details. The most significant enhancement of the amplitude ensured by graphene oxide was stated. Considering biocompatibility of the both types of carbon-based nanomaterials, they can be potentially used in future as contrast agents for bio-imaging and theranostic applications.

Keywords — laser ultrasound; photoacoustics; phantom tissue; carbon nanoparceiles

I. INTRODUCTION

Laser ultrasound imaging based on photoacoustic effect is an emerging diagnostic technique ensuring high resolution, real-time and depth-resolved visualization of biological tissues [1]–[3]. Photoacoustic effect refers to light radiation absorption by a matter with subsequent conversion of the accumulated energy into heat as a result of non-radiative relaxation of the photoexcitation. Acoustic waves (laser ultrasound) generated through thermoelastic expansion of the matter can be further detected by broadband ultrasonic transducers. Photoacoustic imaging combines high spatial

resolution of ultrasonic imaging and high contrast of optical imaging [4]. Compared to other high-resolution volumetric optical imaging modalities widely used in the biomedical imaging field, including confocal microscopy and two-photon microscopy, which suffer from the limitation of depth less than 1 mm, photoacoustic imaging can overcome the limitation of depth and be detected up to a few centimeters deep in biological tissues [5]–[7]. In addition, because photoacoustic signal is mainly determined by photothermal

conversion, the principles of selecting agents for imaging are naturally consistent with those for photothermal therapy, which makes photoacoustic and photothermal therapy an ideal pair to be seamlessly combined into theranostics application. Furthermore, the advantages of photoacoustic imaging involve real-time imaging in vivo and high spatial resolution without the use of ionizing radiation [8].

Meanwhile, photoacoustic contrast agents can enhance the imaging resolution, contrast and depth of detection [9]–[11]. Such contrast agents should satisfy the following conditions: outstanding biocompatibility, appropriate stability in vivo, desirable targeting properties. Nanomaterials are promising contrast agents to satisfy the requirements. Nanomaterials provide a platform for theranostic application to concurrently realize therapy and diagnosis [12]–[14].

Carbon nanomaterials have unique physical and attracted increasing attention in the biomedical field [15]. For instance, most of these carbon nanomaterials possess strong absorption in the infrared or near infrared regions, which is useful for photothermal therapy of cancer [16], [17]. Carbon

Marie Skłodowska-Curie Research and Innovation Staff Exchange program (proposal #690945)

Ministry of Science and Education of Ukraine, Ukraine (State registration number of the project is 0118U000242)

nanomaterials have been used as optical agent in biological imaging such as Raman microscopy [18], [19], fluorescence imaging [20], [21] and photoacoustic imaging [22]–[24]. The main advantages of carbon nanomaterials for their biomedical applications are fully biocompatibility, low toxicity, easy penetration through cells, photoluminescence features [21], [25]–[29].

Study of laser-ultrasound generation efficiency with different nanoparticles is an important step for their further use in *ex/in-vivo* diagnostics [14], [30]. In addition, their preliminary testing on bio-phantoms simulating properties of living object is essential. A large number of phantoms have been already developed to mimic optical and acoustic properties of biological tissues. Phantom studies allow systematic testing and optimization of new methods in a controlled way, before their direct applications to animals and humans. Phantoms are also used to compare performances of photoacoustic imaging, ultrasound systems as well as to assist in the development of new acoustic, ultrasound transducers, systems or diagnostic techniques. The advantages of phantoms is that the idealized tissue models can be constructed with well-defined acoustic properties, dimensions and internal features, thereby simplifying and standardizing the imaging environment [31]. In particular, agarose is a biocompatible polysaccharide polymer material which can be easily prepared and is widely used as a basic material to mimic soft living tissues for magnetic resonance, ultrasound and photoacoustic imaging [31]–[34].

Our communication is devoted to photoacoustic characterization of agarose-based phantoms with use of carbon nanomaterials as photoacoustic contrast agents. Laser ultrasound formation in the phantoms doped with the nanoparticles has been studied. Acoustic response as a function of nano-carbon concentration was detected with a piezoelectric transducer. A significant enhancement of the detected laser-induced acoustic signal emitted by the agarose phantoms has been stated.

II. MATERIALS AND METHODS

A. Phantom tissue preparation

The agarose gel is widely used as a phantom of human tissue because its acoustic characteristics are similar to those of numerous human body parts [35]. For example, the gel with agarose concentrations lower than 4% has properties similar to that of soft tissue, such as: breast, brain, liver, kidney, while the gels with higher agarose concentrations has a microstructure similar to hard tissue [36]. The soft tissues are composed of muscles, tendons, ligaments, fascia, fat, fibrous tissue, synovial membranes, nerves and blood vessels. The hard tissues are mineralized with a firm intercellular substance and include cortical bone, trabecular bone, dental enamel and dentin [31].

In our work, gels with 2 w/v% agarose concentrations have been prepared to mimic soft tissues with a simple homogeneous internal structure [37]–[39]. Two types of agarose-based phantom samples were prepared for our

measurements: pure agarose gel without any added contrast agents, and agarose gels doped with carbon nanomaterials [40], [41].

Agarose phantoms preparation procedure includes the following steps. A solution of agarose powder (A9539, Sigma Aldrich) was dissolved in water, heated to 95°C, and stirred for 30 min to form a gel. Colloids with photoacoustic contrast agents were firstly heated to gel temperature. Then colloids added to the agarose solution and stirred for 10 min. The solution was poured into a mold. Then, it was left for cooling and solidification for 24 hours at room temperature. The gel was then removed from the mold. The phantom samples were prepared as 5 mm thick cylinders with 30 mm in diameter.

Reduced graphene oxide (805424, Sigma Aldrich) and detonation nanodiamonds were chosen as photoacoustic sensitizers. Solid state powders of detonation nanodiamonds were provided by Ray Techniques Ltd. The carbon-based nanomaterials have been thermally oxidized by heating in air at 420 ° C for 1 hour. After that, dispersed in water by a simple stirring (without using any surfactant) and additionally ultrasonicated in a bath-type system.

B. Experimental setup

The used experimental setup is shown schematically in Fig. 1. The second harmonic (532 nm) light radiation from a Q-switched Nd:YAG laser with a 20 ns pulse duration was used as an excitation source. Pulse energy was reduced by a filter to avoid any sample damage. Additionally, the intensity of the laser beam was controlled with a photodiode. The beam

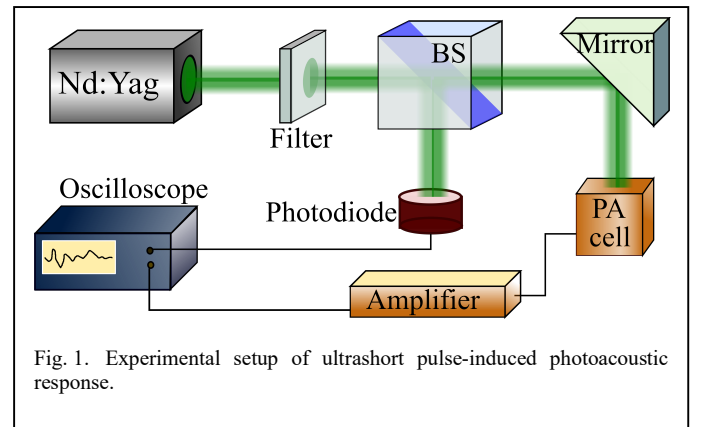


Fig. 1. Experimental setup of ultrashort pulse-induced photoacoustic response.

was directed toward a photoacoustic probe shown in Fig. 2.

The photoacoustic probe was specially designed for ultrasound response detections. Sketch of the probe is shown schematically in Fig. 2. It consists of a transparent buffer (30 mm thick glass piece) and a piezoelectric sensor being in rigid contact with the buffer. The piezoelectric transducer with a ring shape have outer/inner diameters and thickness equal to 10/20 mm and 1 mm, respectively. The photoacoustic probe contacts the phantom sample through a transmission gel. Generated photoacoustic signals were detected by a digital oscilloscope. The final oscillogram was averaged among 128 pulses.

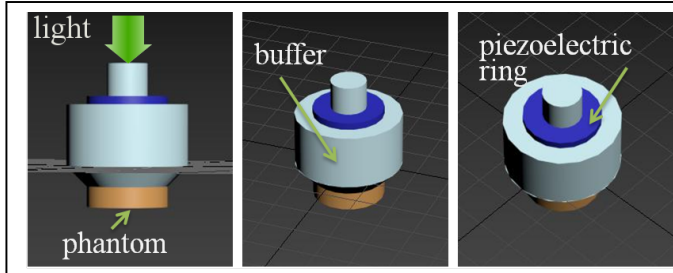


Fig. 2. Schematic configuration of photoacoustic probe with studied phantom.

III. RESULTS AND DISCUSSIONS

A typical signal waveforms detected from agarose phantoms with different concentration of nanodiamonds are shown in Fig. 3. Peak-to-peak amplitude of the photoacoustic signal was measured as a function of the nanodiamond concentration varying from 0.01% w/v to 1%w/v. As one can see in Fig. 3, the experimental amplitude rises with the increase of the nanodiamond concentration.

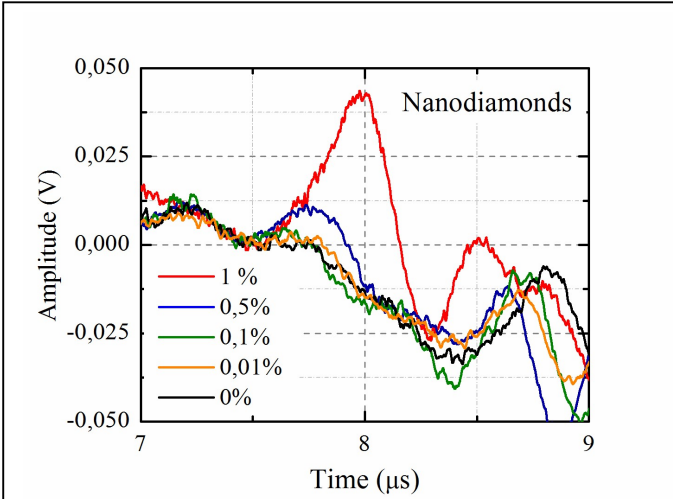


Fig. 3. Laser ultrasound responses for agarose phantoms with different concentration of nanodiamonds

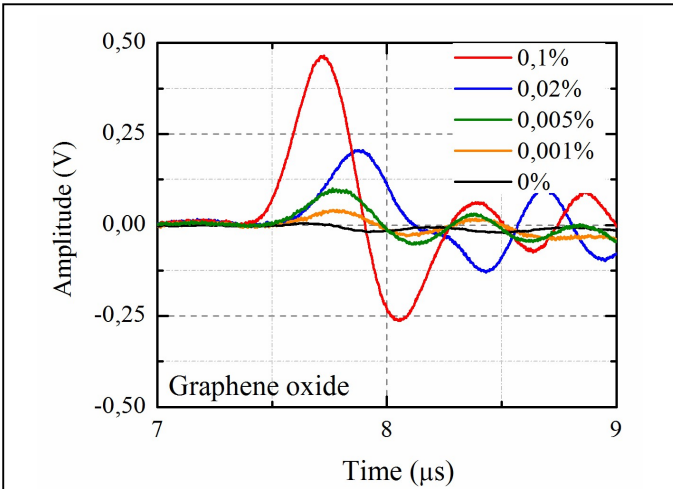


Fig. 4. Laser ultrasound responses for agarose phantoms with different concentration of graphene oxide

Laser ultrasound responses of the agarose phantoms with different concentration of graphene oxide are shown in Fig. 4. The concentration of graphene oxide was one order of magnitude lower (from 0.001% w/v to 0.1%w/v) than in the case of nanodiamond particles. As it can be seen in Fig. 4, the continuously growing signal amplitude is one order of magnitude higher compared to the case of nanodiamonds. The concentration dependencies of the laser ultrasound amplitude for the agarose-based phantom tissues with graphene oxide and nanodiamonds particles are compared in Fig. 5.

This figure demonstrates a non-linear rising of the experimental values of amplitude with the increase of the carbon nanomaterials concentration. For comparison, amplitude of laser ultrasound response of the nanoparticles free agarose phantom tissue was equal to 0.01 V. Thus, application of graphene oxide as a photoacoustic contrast agent will lead to the more important enhancement of laser-induced ultrasound response in comparison with the nanodiamond particles. Amplitude of laser ultrasound response of agarose phantom tissue with minimal

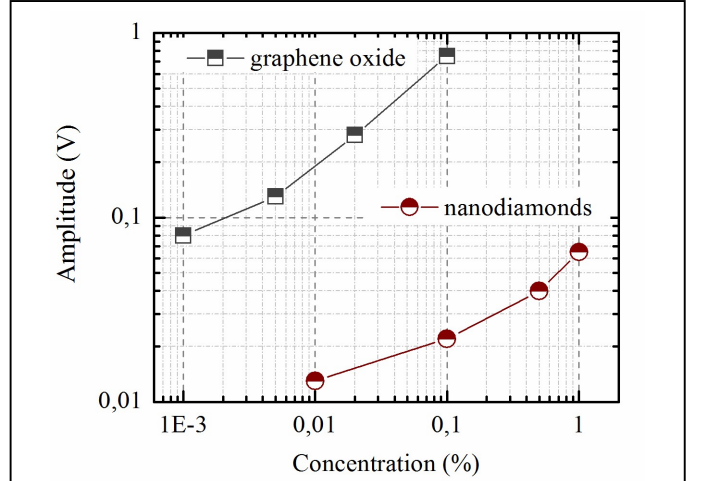


Fig. 5. Concentration dependencies of laser ultrasound response amplitude for agarose-based phantom tissues with carbon nanomaterials

concentration of graphene oxide (0.001%) is almost the same as the amplitude from agarose phantom with maximal concentration (1%) of the nanodiamonds. It should be noted that the concentration of nanoparticles on the one hand should be sufficient to register a stable laser ultrasound signal, but on the other hand should not be toxic to biological objects in which these nanoparticles are injected. In our experiments minimum of nanomaterials concentration which was detected satisfies the both conditions [42]–[45].

CONCLUSIONS

Laser ultrasound enhancement in a phantom tissue doped with carbon nanomaterials (nanodiamonds and graphene oxide) was studied with the use of a pulsed laser excitation (532 nm). The phantoms based on agarose gel were prepared to mimic properties of soft biological tissues. Special

acoustical probe with built-in piezoelectric transducer was applied for the ultrasound detection. Dependencies of the laser ultrasound amplitude on concentration of the carbon nanomaterials incorporated into the phantom tissues were measured. A significant enhancement of the amplitude induced by presence of carbon nanomaterials can be stated. It was found, that application of graphene oxide as photoacoustic contrast agent leads to a much more efficient laser ultrasound response enhancement in comparison with nanodiamonds. Finally, taking into account excellent biocompatibility and low cytotoxic levels of the both nanoparticle types, they can be applied for laser-based cancer theranostics.

ACKNOWLEDGMENT

This research work has been carried out in frames of CARTHER project (proposal #690945) of Marie Skłodowska-Curie Research and Innovation Staff Exchange program.

The publication contains the research results obtained in the framework of the research work "Features of photothermal and photoacoustic processes in low-dimensional semiconductor systems based on silicon" (state registration number 0118U000242).

REFERENCES

- [1] A. S. Hannah, D. Vanderlaan, Y. Chen, and S. Y. Emelianov, "Photoacoustic and ultrasound imaging using dual contrast perfluorocarbon nanodroplets triggered by laser pulses at 1064 nm," *Biomed Opt Express*, vol. 5, no. 9, pp. 3042–3052, 2014.
- [2] M. J. Stevenson and M. C. He, "Sounding Out Dysfunctional Oxygen Metabolism: A Small-Molecule Probe for Photoacoustic Imaging of Hypoxia," *Biochemistry*, vol. 57, pp. 893–894, 2018.
- [3] A. P. Jathoul, J. Laufer, O. Ogunlade, B. Treeby, B. Cox, E. Zhang, P. Johnson, A. R. Pizzey, B. Philip, T. Marafioti, M. F. Lythgoe, R. B. Pedley, M. A. Pule and P. Beard, "Deep in vivo photoacoustic imaging of mammalian tissues using a tyrosinase-based genetic reporter," *Nat Photonics*, vol. 9, pp. 239–246, 2015.
- [4] M. Xu and L. V. Wang, "Photoacoustic imaging in biomedicine," *Rev Sci Instrum*, vol. 77, no. 41101, pp. 1–22, 2006.
- [5] V. Ntziachristos, "Going deeper than microscopy: the optical imaging frontier in biology," *Nat Methods*, vol. 7, pp. 603–614, 2010.
- [6] J. A. Copland, M. Eghtedari, V. L. Popov, N. Kotov, N. Mamedova, M. Motamedi, and A. A. Oraevsky, "Nanoparticles as a Molecular Based Contrast Agent: Implications for Imaging of Deep Tumors Using Photoacoustic Tomography," *Mol Imaging Biol*, vol. 6, no. 5, pp. 341–349, 2004.
- [7] G. Ku and L. V. Wang, "Deeply penetrating photoacoustic tomography in biological tissues enhanced with an optical contrast agent," *Opt Lett*, vol. 30, no. 5, pp. 507–509, 2005.
- [8] X. Wang and L. V. Wang, "Noninvasive imaging of hemoglobin concentration and oxygenation in the rat brain using high-resolution photoacoustic tomography," *J Biomed Opt*, vol. 11, no. April 2006, pp. 1–9, 2006.
- [9] Z. Zha, Z. Deng, Y. Li, C. Li, J. Wang, S. Wang, E. Qu and Z. Dai, "Biocompatible polypyrrole nanoparticles as a novel organic photoacoustic contrast agent for deep tissue imaging," *Nanoscale*, vol. 5, no. April, pp. 4462–4467, 2013.
- [10] K. L. and Bin Liu, "Polymer-encapsulated organic nanoparticles for fluorescence and photoacoustic imaging," *Chem Soc Rev*, vol. 43, pp. 6570–6597, 2014.
- [11] D. Pan, B. Kim, L. V. Wang, and G. M. Lanza, "A brief account of nanoparticle contrast agents for photoacoustic imaging," *Wiley Interdiscip Rev Nanomed Nanobiotechnol*, vol. 5, no. 517, 2013.
- [12] B. Sumer and J. Gao, "Theranostic nanomedicine for cancer," *Nanomedicine*, vol. 3, no. 2, pp. 137–140, 2008.
- [13] J. Rosenholm and V. Mamaeva, "Nanoparticles in targeted cancer therapy: mesoporous silica nanoparticles entering preclinical development stage," *Nanomedicine*, vol. 7, no. 1, pp. 111–120, 2014.
- [14] H. Peng, X. Liu, G. Wang, M. Li, K. M. Bratlie, and E. C. and Q. Wang, "Polymeric Multifunctional Nanomaterials for Theranostics Polymeric multifunctional nanomaterials for theranostics," *J Mater Chem B*, vol. 3, no. July, pp. 6856–6870, 2015.
- [15] Z. Liu and X. J. Liang, "Nano-carbons as theranostics," *Theranostics*, vol. 2, no. 3, pp. 235–237, 2012.
- [16] B. Kang, D. Yu, Y. Dai, S. Chang, D. Chen, and Y. Ding, "Cancer-Cell Targeting and Photoacoustic Therapy Using Carbon Nanotubes as 'Bomb' Agents," *Small*, vol. 5, no. 11, pp. 1292–1301, 2009.
- [17] J. Zhong, S. Yang, X. Zheng, T. Zhou, and D. Xing, "In vivo photoacoustic therapy with cancer-targeted indocyanine green-containing nanoparticles," *Nanomedicine*, vol. 8, no. 6, pp. 903–919, 2013.
- [18] Z. Liu, X. Li, S. M. Tabakman, K. Jiang, S. Fan, and H. Dai, "Multiplexed Multicolor Raman Imaging of Live Cells with Isotopically Modified Single Walled Carbon Nanotubes," *J Am Chem Soc*, vol. 130, no. 41, pp. 13540–13541, Oct. 2008.
- [19] Z. Liu, C. Davis, W. Cai, L. He, X. Chen, and H. Dai, "Circulation and long-term fate of functionalized, biocompatible single-walled carbon nanotubes in mice probed by Raman spectroscopy," *Proc Natl Acad Sci*, vol. 105, no. 5, p. 1410 LP-1415, Feb. 2008.
- [20] C. H. Lee, R. Rajendran, M.-S. Jeong, H. Y. Ko, J. Y. Joo, S. Cho, Y. W. Chang, S. Kim, "Bioimaging of targeting cancers using aptamer-conjugated carbon nanodots," *Chem Commun*, vol. 49, no. 58, pp. 6543–6545, 2013.
- [21] H. D. K. Welsher, Z. Liu, S.P. Sherlock, J.T. Robinson, Z. Chen, D. Daranciang, "A route to brightly fluorescent carbon nanotubes for near-infrared imaging in mice," *Nat Nanotechnol*, vol. 4, pp. 773–780, 2009.
- [22] S. S. Gambhir, A. De La Zerda, C. Zavaleta, S. Keren, S. Vaithilingam, S. Bodapati, Z. Liu, J. Levi, B.R. Smith, T.-J. Ma, O. Oralkan, Z. Cheng, X. Chen, H. Dai, B.T. Khuri-Yakub, "Carbon nanotubes as photoacoustic molecular imaging agents in living mice," *Nat Nanotechnol*, vol. 3, no. 557–562, 2008.
- [23] A. de la Zerda, J. W. Kim, E. I. Galanzha, S. S. Gambhir, and V. P. Zharov, "Advanced contrast nanoagents for photoacoustic molecular imaging, cytometry, blood test and photothermal theranostics," *Contrast Media Mol Imaging*, vol. 6, no. 5, pp. 346–369, 2011.
- [24] V. P. Zharov, J.-W. Kim, E.I. Galanzha, E.V. Shashkov, H.-M. Moon, "Golden carbon nanotubes as multimodal photoacoustic and photothermal high-contrast molecular agents," *Nat Nanotechnol*, vol. 4, pp. 688–694, 2009.
- [25] Y. Liu, D. Yu, C. Zeng, Z. Miao, and L. Dai, "Biocompatible Graphene Oxide-Based Glucose Biosensors," *Langmuir Lett*, vol. 26, no. 19, pp. 6158–6160, 2010.
- [26] X. Sun, Z. Liu, K. Welsher, J. T. Robinson, A. Goodwin, and S. Zaric, "Nano-Graphene Oxide for Cellular Imaging and Drug Delivery," *Nano Res*, vol. 1, pp. 203–212, 2008.
- [27] A. M. Schrand, L. Dai, J. J. Schlager, S. M. Hussain, and E. Osawa, "Differential biocompatibility of carbon nanotubes and nanodiamonds," *Diam Relat Mater*, vol. 16, no. 12, pp. 2118–2123, 2007.
- [28] C. Grabinski, S. Hussain, K. Lafdi, L. Braydich-Stolle, and J. Schlager, "Effect of particle dimension on biocompatibility of carbon nanomaterials," *Carbon N Y*, vol. 45, no. 14, pp. 2828–2835, 2007.
- [29] Y.-K. Kim, M.-H. Kim, and D.-H. Min, "Biocompatible reduced graphene oxide prepared by using dextran as a multifunctional reducing agent," *Chem Commun*, vol. 47, no. 11, pp. 3195–3197, 2011.
- [30] H. Von Tengg-kobligh and U. Bern, "3D printing based on imaging data: Review of medical applications," *Int J Comput Assist Radiol Surg*, vol. 5, pp. 335–341, 2010.
- [31] M. Culjat, D. Goldenberg, P. Tewari, and R. Singh, "A review of tissue substitutes for ultrasound imaging," *Ultrasound Med Biol*, vol. 36, no. 6, pp. 861–873, 2010.

- [32] A. Józefczak, K. Kaczmarek, M. Kubovčíková, Z. Rozynek, and T. Hornowski, "The effect of magnetic nanoparticles on the acoustic properties of tissue-mimicking agar-gel phantoms," *J Magn Magn Mater*, vol. 431, pp. 172–175, 2017.
- [33] M. R. Fisher, N. S. Nogar, and S. M. Schuster, "Pulsed optoacoustic spectroscopy of NADH," *Anal Biochem*, vol. 113, no. 1, pp. 112–117, 1981.
- [34] P. Zarrintaj, S. Manouchehri, Z. Ahmadi, M. R. Saeb, A. M. Urbanska, D. L. Kaplan, M. Mozafari, "Agarose-based biomaterials for tissue engineering," *Carbohydr Polym*, vol. 187, pp. 66–84, 2018.
- [35] T. D. Mast, "Empirical relationships between acoustic parameters in human soft tissues," *Acoust Res Lett Online*, vol. 1, pp. 37–42, 2000.
- [36] M. Salloum, R. H. Ma, D. Weeks, and L. Zhu, "Controlling nanoparticle delivery in magnetic nanoparticle hyperthermia for cancer treatment: experimental study in agarose gel," *Int J Hyperth*, vol. 24, pp. 337–345, 2008.
- [37] F. Adams, T. Giu, A. Mark, B. Fritz, L. Kramer, D. Schlager, U. Wetterauer, A. Miernik, P. Fischer, "Soft 3D-Printed Phantom of the Human Kidney with Collecting System," *Ann Biomed Eng*, vol. 45, no. 4, pp. 963–972, 2017.
- [38] N. I. Niebuhr, W. Johnen, T. Güldaglar, A. Runz, G. Echner, P. Mann, C. Möhler, A. Pfaffenberger, O. Jäkel, and S. Grelich, "Technical Note: Radiological properties of tissue surrogates used in a multimodality deformable pelvic phantom for MR-guided radiotherapy" *Med Phys*, vol. 43, no. 2, pp. 907–916, 2016.
- [39] S. S. Alvarez, L. F. E. Huerta, A. V. Vargas, J. López, J. G. Silva, and C. A. González, "Characterization of Breast Cancer Radiofrequency Ablation Assisted with Magnetic Nanoparticles: In Silico and in Vitro Study," *J Electromagn Anal Appl*, vol. 8, pp. 1–7, 2016.
- [40] J. Tucker - Schwartz, T. Hong, D. C Colvin, Y.-Q. Xu, and M. Skala, Dual Modality Photothermal Optical Coherence Tomography and Magnetic Resonance Imaging of Carbon Nanotubes, *Optics letters*, vol. 37, pp.872-874, 2012.
- [41] Y.-W. Wang, Y.-Y. Fu, Q. Peng, S.-S. Guo, G. Liu, J. Li, H.-H. Yang, G.-N. Chena, "Dye-enhanced graphene oxide for photothermal therapy and photoacoustic imaging," *J Mater Chem B*, vol. 1, pp. 5762–5767, 2013.
- [42] A. B. Seabra, A. J. Paula, R. De Lima, and O. L. Alves, "Nanotoxicity of Graphene and Graphene Oxide," *Chem Res Toxicol*, vol. 27, no. 2, pp. 159–168, 2014.
- [43] L. Zhang, J. Xia, Q. Zhao, L. Liu, and Z. Zhang, "Functional Graphene Oxide as a Nanocarrier for Controlled Loading and Targeted Delivery of Mixed Anticancer Drugs," *Small*, vol. 6, no. 4, pp. 537–544, 2010.
- [44] Y. Chang, S.-T. Yang, J.-H. Liu, E. Dong, Y. Wang, A. Cao, Y. Liu, H. Wang, "In vitro toxicity evaluation of graphene oxide on A549 cells," *Toxicol Lett*, vol. 200, no. 3, pp. 201–210, 2011.
- [45] I. E. Mej, C. M. Santos, and D. F. Rodrigues, "Nanoscale Toxicity of a polymer – graphene oxide composite against bacterial planktonic," *Nanoscale*, vol. 4, pp. 4746–4756, 2012.